Journal of *Marine Science and Engineering*

MDPI

Article

Ship Speed Optimization Method in Canal Environments Considering Waiting Times for Crossing Locks

Wen Xie [1], Sudong Xu [1,*], Nini Zhang [1], Jun Liu [2], Kai Yin [1] and Liuyan Mao [1]

[1] Department of Port, Waterway and Coastal Engineering, School of Transportation, Southeast University, Nanjing 211189, China; 220213583@seu.edu.cn (W.X.); ninizhang@seu.edu.cn (N.Z.); kyin@seu.edu.cn (K.Y.); cpmly@163.com (L.M.)

[2] North Jiangsu Grand Canal Administration of Navigational Affairs, Huai'an 223001, China; liujunsbc@163.com

* Correspondence: sudongxu@seu.edu.cn

Abstract: The shipping industry faces a pressing challenge with carbon emissions, prompting a focus on speed optimization for energy conservation and emission reduction. While much research has centered on optimizing speeds in oceans and rivers, canals have received less attention, despite their unique challenges of narrow waterways and busy locks. This study fills this gap by establishing a fuel consumption prediction model integrating key environmental factors such as water depth, width, and flow velocity. Drawing upon established methodologies in speed optimization, this study augments these models with waiting time limits for each canal segment. To validate the efficacy of the model, three representative ships are selected as case studies. The findings reveal a high predictive capability of the fuel consumption model, as evidenced by R^2 values exceeding 0.97 across all cases. Notably, the optimization approach yields a fuel consumption reduction ranging from 4% to 5% for short waiting times. Furthermore, compared to conventional methods, the proposed optimization strategy achieves an 8.19% enhancement in fuel consumption and carbon emission reduction for long waiting times, culminating in an overall optimization rate of 11.54%. These results underscore the significance of employing the proposed speed optimization methodology, particularly during peak periods of canal congestion.

Keywords: speed optimization; fuel consumption; canals; waiting time; water depth

check for updates

Citation: Xie, W.; Xu, S.; Zhang, N.; Liu, J.; Yin, K.; Mao, L. Ship Speed Optimization Method in Canal Environments Considering Waiting Times for Crossing Locks. *J. Mar. Sci. Eng.* **2024**, *12*, 375. https://doi.org/10.3390/jmse12030375

Academic Editor: Mihalis Golias

Received: 15 January 2024
Revised: 9 February 2024
Accepted: 20 February 2024
Published: 22 February 2024

Copyright: © 2024 by the authors. Licensee MDPI, Basel, Switzerland. This article is an open access article distributed under the terms and conditions of the Creative Commons Attribution (CC BY) license (https://creativecommons.org/licenses/by/4.0/).

1. Introduction

In response to the pressing need to address global warming, extensive efforts have been undertaken worldwide to mitigate greenhouse gas emissions. Notably, in 2021, the European Union (EU) introduced the "European Climate Law", delineating ambitious emission reduction targets for the subsequent three decades [1]. Concurrently, the United States unveiled its comprehensive strategy, titled "The Long-Term Strategy of the United States: Pathways to Net-Zero Greenhouse Gas Emissions by 2050" [2]. Likewise, the Chinese government outlined its objectives concerning "carbon peaking and carbon neutrality" as pivotal strategies to manage and reduce carbon emissions [3]. These initiatives underscore the global commitment to addressing climate change through proactive measures and policy interventions.

Carbon emissions within the shipping sector have garnered significant attention from the international community, posing a substantial challenge for achieving green transformation in the global shipping industry [4–6]. In response to the pressing need for action against climate change, the International Maritime Organization (IMO) adopted "The Initial GHG Strategy" for International Shipping in 2018, delineating greenhouse gas (GHG) reduction targets for the industry [7]. Concurrently, initiatives such as "The Getting to Zero Coalition" have emerged to foster collaboration within the industry toward the development of zero-emission vessels [8]. Notably, carbon emissions in shipping are closely

linked to fuel consumption, presenting shipping companies with the dual challenge of reducing environmental impact while navigating escalating global fuel prices [9]. Thus, in addressing both environmental and economic considerations, the imperative task emerges of minimizing fuel consumption and carbon emissions. Such endeavors not only advance environmentally sustainable shipping practices, but also align with the objectives of cost reduction and profit maximization for shipping enterprises.

Relevant research on reducing ship fuel consumption predominantly concentrates on two key areas: design optimization and operational optimization. Among these, technology optimization stands out as both technically intricate and financially demanding. Operational optimization encompasses various strategies such as route optimization [10–12], energy management [13–15], and speed optimization [16–18]. Unlike maritime transport, where routes are often flexible, inland water transport routes tend to be relatively fixed, limiting optimization possibilities. Additionally, vessels operating in confined waterways exhibit diverse sizes, including numerous small, independently owned ships. Consequently, efforts to optimize ship engine efficiency may not yield widespread benefits in such constrained environments. Hence, speed optimization emerges as an efficient, convenient, and universally applicable approach for enhancing energy efficiency in restricted waterways.

Currently, research on speed optimization predominantly centers on oceanic [18,19] and natural river environments [17,20,21], with limited exploration in canal settings. As the construction and development of inland ports and waterways persist, water transport is increasingly utilized for inland transportation [22]. Canals, in particular, have emerged as vital components of inland water transport networks. Furthermore, ship speed significantly influences fuel consumption, underscoring the importance of optimizing fuel consumption in canal navigation. Canals are artificial waterways characterized by narrow cross-sections and distinct navigational constraints for ships and fleets [23]. Unlike oceans and natural rivers, canals exhibit the following unique characteristics:

- Narrow waterway. The confined waterway, characterized by regular section shapes, flat riverbeds, and steady flows, plays a significant role in determining the resistance encountered by vessels navigating canals [24]. Due to the higher resistance encountered by a ship of the same dimensions navigating canals compared to natural rivers [25], the speeds of canal vessels are considerably restricted.
- Busy locks. Locks serve as crucial mechanisms for facilitating smooth navigation along canals. However, due to their limited capacity, congestion of canal vessels frequently occurs during peak seasons. The time spent waiting for and passing through locks constitutes a critical factor influencing the total voyage duration of vessels.

Ship resistance stands as a pivotal factor influencing speed, while time serves as a crucial constraint in speed optimization models [20,21]. In light of the distinctive characteristics of canals outlined earlier, this paper endeavors to develop a model for ship fuel consumption within canal environments. Furthermore, this study explores a ship speed optimization approach that incorporates waiting times for vessels to navigate locks. The objective is to mitigate fuel consumption and carbon emissions in canal transportation.

The primary contributions of this paper are as follows:

- The establishment of a ship fuel consumption prediction model tailored to canal environmental conditions, incorporating waterway depth, width, and water flow velocity as key influencing factors.
- The integration of waiting time constraints into the speed optimization model, addressing the unique booking characteristics associated with ship passage through locks.
- A comparative analysis of three cases to evaluate the fuel consumption optimization efficacy of the proposed speed optimization method compared to conventional approaches.

This paper is structured as follows: Section 2 delves into the existing advancements in fuel consumption prediction and identifies research gaps within speed optimization.

Section 3 delves into the modeling methodologies employed for prediction and optimization purposes. Section 4 offers insights into the case background, operational conditions, outcomes, and subsequent discussion. Finally, Section 5 provides a comprehensive summary of the paper's findings and contributions.

2. Literature Review

2.1. Ship Fuel Consumption Prediction

The objective of speed optimization research is to minimize a ship's fuel consumption by identifying the optimal speed. The development of an accurate and efficient prediction model for ship fuel consumption serves as a foundational element in speed optimization research [26,27]. The precision of the ship fuel consumption prediction model is influenced by environmental factors and the selection of the prediction model.

The interaction between ship propulsion systems and the environment underscores the importance of selecting appropriate environmental factors in fuel consumption optimization studies [21]. Environmental conditions directly impact ship fuel consumption through factors like ship resistance [20]. In oceanic environments, predominant environmental factors include wind, waves, and ocean currents [25]. Conversely, inland rivers are influenced by water depth, wind, waves, and flow. Fan et al. [21] highlighted water flow and waterway depth as primary factors affecting fuel consumption in inland shipping, while Yan et al. [20] investigated energy-efficient speeds, considering the impact of wind, waves, and water depth. Li et al. [28] focused on ship speed optimization with regard to weather conditions. Moreover, numerous studies have demonstrated the significant impact of canal width and depth on vessel resistance [24,29,30]. For instance, Hadi et al. [24] explored the influence of canal dimensions on the resistance of a 750 DWT ship, noting the heightened sensitivity of faster vessels to changes in waterway constraints. Therefore, this research prioritizes waterway depth and width as primary environmental factors while also considering the effects of water flow velocity.

Existing ship fuel consumption prediction models can be categorized into three primary types based on their deductibility [31,32]. White-box models, such as those derived from theoretical knowledge [26,33], offer good interpretability but may have limited predictive capabilities. Black-box models, which rely on historical data for training [27,34], provide high predictive accuracy but require extensive historical data and lack transparency in their internal workings. Grey-box models, which combine theoretical knowledge-based model structures with parameter estimation through historical data [35], offer a balance of accuracy and interpretability.

Accessing historical voyage data for canal vessels poses a challenge due to the absence of Voyage Data Recorders (VDRs) in some vessels, particularly private ones that may not prioritize data recording. To mitigate this limitation, the proposed framework of the ship fuel consumption prediction model in this paper employs a combination of white-box and grey-box models. The white-box model is utilized to reduce the data requirement, leveraging theoretical knowledge to enhance interpretability. Meanwhile, the grey-box model is employed to refine the regression of the engine power and fuel consumption rate, thereby enhancing the accuracy of the prediction model. This approach aims to strike a balance between data availability and model accuracy.

2.2. Ship Speed Optimization

The current research objectives in ship speed optimization can be categorized into three main areas: maximizing total profit [28], minimizing total emissions [16], and addressing the dual objectives of profit and emissions [36,37]. Given that ship emissions are directly linked to fuel consumption, efforts to minimize total emissions can also be interpreted as attempts to minimize total fuel consumption. The outcome of such optimization efforts typically involves determining optimal speeds for various segments [38].

The research problem addressed in this paper revolves around computing the optimal speed solution for each segment to minimize total fuel consumption under specified con-

straints. Previous studies have employed various optimization algorithms to tackle similar problems. For instance, Liu et al. [28] utilized the NSGA-II algorithm to solve a bi-objective optimization problem involving ship speed and EEOI (Energy Efficiency Operational Indicator). Yan et al. [20] applied the PSO (Particle Swarm Optimization) algorithm to calculate optimal speeds for fuel consumption minimization. Fan et al. [21] employed dynamic programming to address speed optimization by dividing shipping speed into different gears. Zhang et al. [38] utilized augmented Lagrangian differential evolution to optimize vessel speeds on the Yangtze River. Given the multivariate nature of this optimization problem, there is a risk of converging to local optimal solutions and potentially missing the global optimum. Genetic algorithms are well suited for global optimization due to their stochastic nature, which includes crossover and mutation operations. Therefore, this paper selects the genetic algorithm as the optimization technique for the speed optimization model.

Current speed optimization studies in inland waterways typically employ constraints such as total sailing time limits and upper and lower speed limits [20,21,39]. However, these studies primarily focus on oceanic and natural river environments. The waiting time for ships at locks in each navigation section is often overlooked as a constraint. Nevertheless, given the bustling nature of canal locks and their proximity to neighboring locks, the duration of ship waiting times significantly influences speed decisions. Moreover, the uncertainty surrounding waiting and crossing times prevents shipowners from devising precise voyage schedules.

Therefore, this study accounts for the distinct waiting time characteristics of different ships and integrates waiting time and crossing time into the speed optimization model. This integration aims to derive more reasonable optimized speeds that better reflect the operational realities of canal navigation.

3. Methodology

3.1. Problem Description

Fuel consumption represents a significant portion of shipping costs, while voyage duration directly impacts operational expenses. While reducing navigation speed can decrease fuel consumption, it simultaneously prolongs voyage times. Notably, the waiting time for canal ships to navigate multi-stage locks substantially influences the total voyage duration and the time allocation for each voyage segment. Constraining the speed optimization model solely by total navigation period may result in the inefficient use of sailing time and increased fuel consumption. Therefore, it becomes imperative to develop a speed optimization model that accounts for waiting times at locks in each navigation segment, leveraging the fuel consumption prediction model tailored to canal environments. The assumptions of the calculation model in this paper are as follows.

1. In the calculation process of the ship fuel consumption model, ship resistance disregards the effects of waves, wind, and biological fouling. Additionally, the shallow-water effect does not influence the open-water characteristics of the propeller.
2. Due to the uncertainty of whether the auxiliary machinery will be turned on when the ship is moored, we have not considered the fuel consumption caused by auxiliary engines during the waiting time in our analysis.
3. The ship maintains a constant speed across different navigation sections.
4. After passing through a lock, a ship can schedule its passage through the next lock. The lock prioritizes ship passages based on reservation order, ensuring consistent transit times for different ships at various locks.
5. Waiting time for crossing a lock refers to the duration between completing the vessel's booking and receiving a notification of lock crossing.
6. If a vessel can reach the next lock on time by sailing at the most fuel-efficient speed or has extra time available, it will finalize the crossing reservation within a fixed period after crossing. If reaching the next lock on time is not feasible at the most fuel-efficient speed, the ship will schedule a crossing reservation for the next lock at the appropriate time, thereby minimizing delays and idle time.

3.2. Fuel Consumption Prediction Model

The resistance of inland ships is typically assessed using the Zwankov formula [40]. However, in restricted waterways where ship resistance is impacted by shallow water and the narrow waterway, modifications to the formula are necessary. Yu et al. [25] adapted the Zwankov formula based on ship resistance model test outcomes, proposing an approximate estimation formula for resistance in restricted waterways. The equation, which accounts for the influence of waterway width and depth on ship resistance, is as follows:

$$R = fSV_s^{1.83} + \frac{0.5SV_s^2\xi(F_h, h/d)}{K_b(L/6b)^3} \tag{1}$$

$$K_b = 0.0995\left(\frac{B}{b}\right)^2 - 1.371\frac{B}{b} + 5.55 \tag{2}$$

$$S = L_\omega(2d + C_B b) \tag{3}$$

where R is the ship resistance (N), f is the friction resistance coefficient, generally taken as 0.17, S is the wet surface area of the hull (m_2), ξ is the residual resistance coefficient, related to the water depth Froude number $F_h = v/\sqrt{gh}$ and the water depth-draft ratio h/d, V_s is the ship speed (m/s), g is the acceleration of gravity (m/s^2), h is the waterway depth (m), d is the ship draft (m), L is the ship length (m), C_B is the ship's block coefficient, $C_B = \Delta/L_\omega bd$, L_ω is the ship waterline length (m), b is the ship width (m), and B is the waterway width (m).

$$\xi\left(F_h, \frac{h}{d}\right) = a_1F_h^3 + a_2F_h^2 + a_3F_h + a_4 \tag{4}$$

$$a_1 = -1118\left(\frac{h}{d}\right)^3 + 6723\left(\frac{h}{d}\right)^2 - 13427\left(\frac{h}{d}\right) + 9010 \tag{5}$$

$$a_2 = 1087\left(\frac{h}{d}\right)^3 - 6517\left(\frac{h}{d}\right)^2 + 12989\left(\frac{h}{d}\right) - 8705 \tag{6}$$

$$a_3 = -388.1\left(\frac{h}{d}\right)^3 + 2331\left(\frac{h}{d}\right)^2 - 4655\left(\frac{h}{d}\right) + 3125 \tag{7}$$

$$a_4 = 47.6\left(\frac{h}{d}\right)^3 - 286.3\left(\frac{h}{d}\right)^2 + 570.4\left(\frac{h}{d}\right) - 378.5 \tag{8}$$

In the above equations, a_1, a_2, a_3, a_4 are coefficients obtained from the regression analysis of ξ and F_h.

The relationship between engine speed and ship speed is pivotal for establishing the link between fuel consumption and speed in subsequent stages. Yan et al. [20] employed the following method for deducing this relationship:

$$J = \frac{V_p}{n_pD} = \frac{(1-\omega)V_s}{i_r \cdot n_eD} \tag{9}$$

$$n_e = \frac{(1-\omega)V_s}{i_rJD} \tag{10}$$

where J is the advance coefficient, ω is the wake coefficient, V_p is the propeller advance speed (km/h), n_p is the propeller speed (r/min), n_e is the ship engine speed (r/min), D is the propeller diameter (m), and i_r is the reduction ratio when the engine and propeller are connected through the gearbox.

Because J and ω vary little with n_e, V_s and n_e can be approximated as a linear relationship:

$$n_e = b_1V_s + b_2 \tag{11}$$

where b_1 and b_2 are the fitting coefficients from Equation (16) and listed in Table A1.

The equations of the thrust coefficient and the torque coefficient are as follows:

$$K_T = \frac{T}{\rho n_p^2 D^4} = f_T(J) \tag{12}$$

$$K_Q = \frac{Q}{\rho n_p^2 D^5} = f_Q(J) \tag{13}$$

where K_T is the thrust coefficient, T is the ship thrust (N), K_Q is the torque coefficient, Q is the ship propeller torque (N·m), and ρ is the water density (kg/m^3).

Based on the relationship between ship resistance and ship thrust in Equation (14), the equation for engine speed is derived, as shown in Equation (16):

$$R = (1-t)T = (1-t)K_T \rho i^2 n_e^2 D^4 \tag{14}$$

$$t = 0.325C_B - 0.1885\frac{D}{\sqrt{bd}} \tag{15}$$

$$n_e = \sqrt{\frac{R}{(1-t)K_T \rho i^2 D^4}} \tag{16}$$

where t is the thrust deduction coefficient.

The equations of engine power and fuel consumption are fitted using the least squares method. The theoretical knowledge construction relationship framework of fuel consumption rate and engine power is as follows. According to Equation (17), the engine power is proportional to the cubic power of the ship engine speed:

$$P_B = \frac{2\pi k \cdot K_Q \rho D^5}{\eta_S \eta_R} \cdot n_e^3 = C_1 n_e^3 \tag{17}$$

where P_B is the main engine power (kW), η_S is shaft transfer efficiency, and η_R is relative rotation efficiency.

The multiple fitting results of the measured data can infer that the fuel consumption rate and engine speed of the marine diesel engine can be fitted by a quadratic polynomial [41].

$$g_e = C_2 n_e^2 + C_3 n_e + C_4 \tag{18}$$

where g_e is the fuel consumption rate of the main engine (g/kWh) and C_1, C_2, C_3, C_4 are the fitting parameters.

The calculation equation of ship fuel consumption for a voyage is as follows:

$$FC = P_e g_e t = C_1 n_e^3 \cdot \left(C_2 n_e^2 + C_3 n_e + C_4\right) \cdot \frac{M}{3.6(V_s + V_w)} \tag{19}$$

where FC is the fuel consumption of a voyage (g), t is the navigation time (h), M is the navigation mileage (km), and V_w is the water flow velocity (m/s).

According to IMO, CO_2 is the main GHG emitted by ship navigation [42]. The estimation formula for ship CO_2 emissions is as follows.

$$CO_2 emission(g) = FC(g) \cdot EF_f(gCO_2/gfuel) \tag{20}$$

where EF_f is the fuel-based emission factor ($gCO_2/gfuel$). Fuel used for restricted-navigation ships is generally Marine Diesel Oil (MDO). Following IMO, the EF_f of MDO is 3.206.

The common evaluation indicators of prediction modeling are as follows:

$$MSE = \frac{1}{n}\sum_{i=1}^{n}(\hat{y}_i - y_i)^2 \tag{21}$$

$$RMSE = \sqrt{\frac{1}{n}\sum_{i=1}^{n}(\hat{y}_i - y_i)^2} \tag{22}$$

$$MAE = \frac{1}{n}\sum_{i=1}^{n}|\hat{y}_i - y_i| \tag{23}$$

$$MAPE = \frac{100\%}{n}\sum_{i=1}^{n}\left|\frac{\hat{y}_i - y_i}{y_i}\right| \tag{24}$$

$$R^2 = 1 - \frac{\sum_{i=1}^{n}(\hat{y}_i - y_i)^2}{\sum_{i=1}^{n}(\bar{y} - y_i)^2} \tag{25}$$

where $\hat{y}_i$ is the predicted value, $\hat{y}_i = \{\hat{y}_1, \hat{y}_2, \ldots, \hat{y}_n\}$, y_i is the real value, $y_i = \{y_1, y_2, \ldots, y_n\}$, $\bar{y}$ is the average value of y_i, MSE is the mean square error, $RMSE$ is the root mean square error, MAE is the mean absolute error, $MAPE$ is the mean absolute percentage error, and R^2 is R-Square. The range of MSE, $RMSE$, and MAE is [0, +∞), which is equal to 0 when the predicted value matches the real value exactly, and the larger the error is, the larger their values are. The range of $MAPE$ is [0%, 100%], and the closer the value is to 0%, the better the prediction is. The range of R^2 is [0, 1], and the closer the value is to 1, the better the prediction is.

3.3. Speed Optimization Model

The mathematical representation of speed optimization using the GA algorithm is as follows. The speed optimization model aims to minimize the total fuel consumption of the entire voyage, considering it to be the objective function in the optimization process. The expression for the total fuel consumption of the entire voyage is as follows:

$$FC_i = C_1 n_{ei}^3 \cdot \left(C_2 n_{ei}^2 + C_3 n_{ei} + C_4\right) \cdot \frac{M_i}{3.6(V_{si} + V_{wi})} \tag{26}$$

$$FC_{total} = \sum_{i=1}^{n} FC_i, \forall i \in \{1, 2, \cdots, n\} \tag{27}$$

where FC_i is the predicted fuel consumption in segment i (g), FC_{total} is the fuel consumption of the ship throughout the whole voyage (g), M_i is the mileage in segment i (km), n_{ei} is the engine speed in segment i (r/min), V_{wi} is the water flow velocity in segment i (m/s), and V_{si} is the ship speed in segment i (m/s).

There are some constraining conditions of the speed optimization model. Fan et al. [21] incorporate speed limits for each segment into the constraint conditions, considering the safety of ship navigation.

$$T_{total} = \sum_{i=1}^{n} \frac{M_i}{3.6 \cdot (V_{si} + V_{wi})} \leq T_{limit}, \forall i \in (1, \ldots, n) \tag{28}$$

$$N_{min} \leq n_{ei} \leq N_{max}, \forall i \in (1, \ldots, n) \tag{29}$$

$$V_{min} \leq V_{si} + V_{wi} \leq V_{max}, \forall i \in (1, \ldots, n) \tag{30}$$

where T_{total} is the total sailing time (h), T_{limit} is the sailing time limit (h), N_{max}, N_{min} are the upper and lower limits of the engine speed (r/min), and V_{max}, V_{min} are the upper and lower limits of the speed in segment i (m/s).

The proposed workflow for the speed optimization model in this paper is depicted in Figure 1. Additionally, the utilization of the GA algorithm for implementing the speed optimization model entails the incorporation of a sailing period division algorithm, outlined in Algorithm 1. The sequential steps of the speed optimization model unfold as follows:

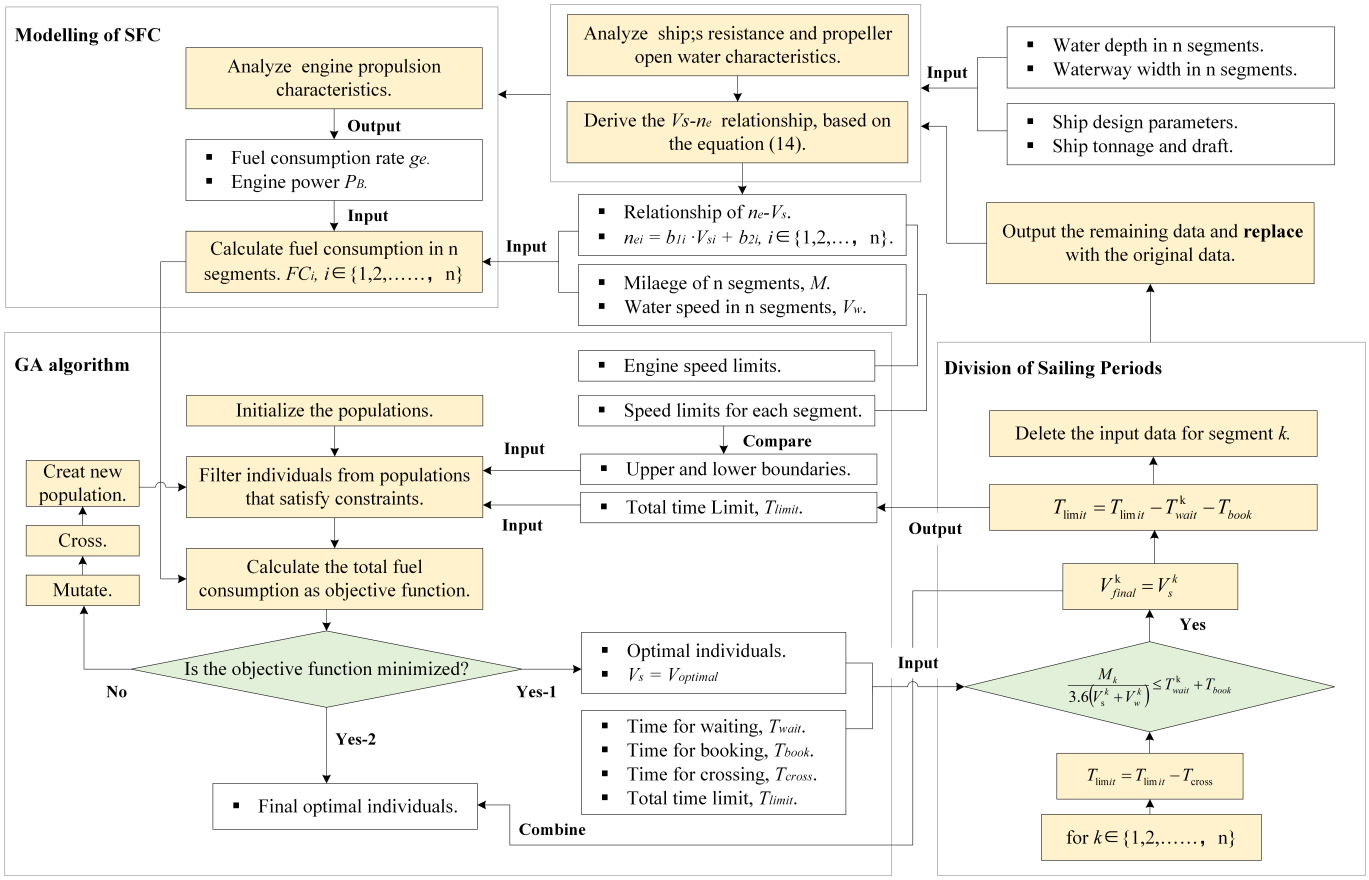

Figure 1. Workflow of the speed optimization model.

Algorithm 1: Sailing period division.

input : $data$—data of n segments; $N = \{1, 2, \cdots, n\}$—set of segment number; $V_{optimal}$—set of optimal individuals calculated by the speed optimization algorithm without time constraints; M—set of mileage of n segments; V_w—set of water flow velocity in n segments; T_{wait}—set of waiting times at n locks; T_{book}—time for booking a lock crossing; T_{cross}—time for crossing a lock; T_{limit}—the limited time of the whole voyage.

output: T_{limit}—limit time of remaining voyage; $data$—remaining data of segments; V_{final}—set of final optimal speed in seg.

$V_s \leftarrow V_{optimal}$;
$seg \leftarrow \{\}$;
for $k \in N$ **do**
  $T_{limit} \leftarrow T_{limit} - T_{cross}$;
  if $M_k/(3.6(V_s^k + V_w^k)) \leq T_{wait}^k + T_{book}$ **then**
    $T_{limit} \leftarrow T_{limit} - T_{wait}^k - T_{book}$;
    $V_{final}^k \leftarrow V_s^k$;
    delete $data$ at segment k;
    else
      $seg \leftarrow seg + \{k\}$;

- Step 1: The initial phase involves fitting the relationship between ship speed and engine speed and modeling ship fuel consumption across n segments, following the methodology detailed in Section 3.2.

- Step 2: Subsequent to fitting and modeling, the GA algorithm is employed to calculate the most fuel-efficient speed for each segment, without imposing a total time constraint.
- Step 3: The sailing period division algorithm, elucidated in Algorithm 1, partitions the segments based on a comparison between waiting time at locks and sailing time at the most fuel-efficient speed. Segments where the waiting time plus booking time exceed the sailing time are excluded, with deductions made from the total time limit.
- Step 4: Finally, a secondary computation of optimal speed is conducted using the GA algorithm, incorporating the remaining data with the total time limit as a constraint. This results in the determination of the final optimal speed for the remaining segments.

4. Case Study

4.1. Case Description

The North Jiangsu Canal, a segment of the Beijing-Hangzhou Canal, boasts favorable navigation conditions, hosts a significant number of ships, and plays a pivotal role in social and economic development [43]. Busy shipping activities are causing an increase in carbon emissions and congestion at the locks on the North Jiangsu Canal. Therefore, the North Jiangsu Canal was chosen as the background for this case study.

Due to the similarity in natural conditions, segmentation in this case study is based on lock locations along the North Jiangsu Canal. Spanning a total length of 404 km, this canal is punctuated by 10 locks positioned along its course. Figure 2 elucidates the distribution of these locks and the waterway direction within the canal. Additionally, Figure 3 illustrates that there is little fluctuation in water depth between adjacent locks, with the majority of the waterway width ranging from 60 to 70 m, although some segments boast widths exceeding 100 m. Notably, a few bottleneck segments exhibit narrower widths below 60 m. Despite these variations, the natural conditions remain largely consistent between neighboring locks. Consequently, the North Jiangsu Canal is segmented into labeled segments ranging from 1# to 11#, corresponding to the ship locks.

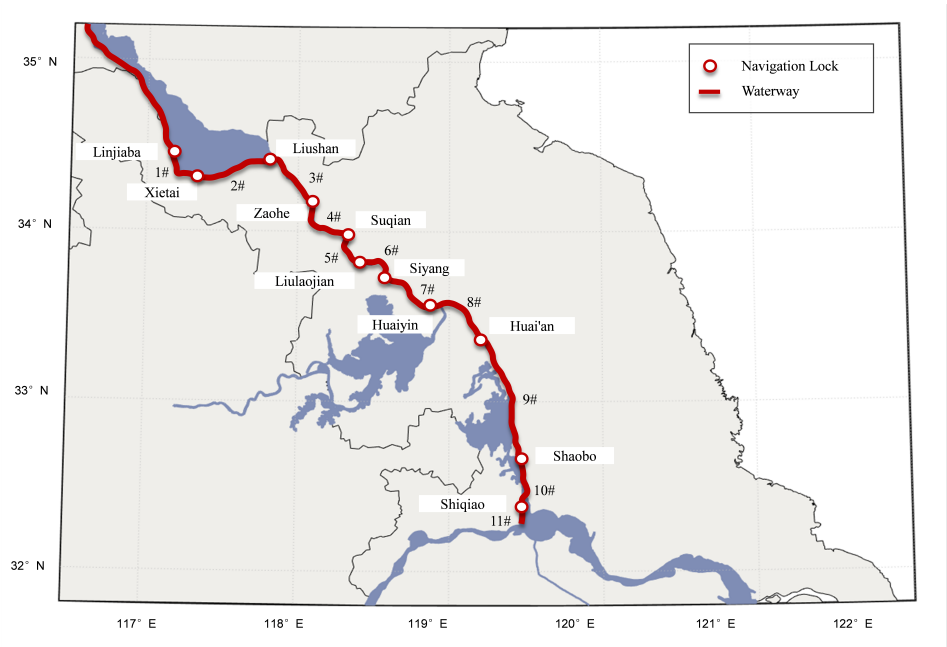

Figure 2. Distribution of locks on the North Jiangsu Canal. (The numbers ranging from 1# to 11# are the labels of segments).

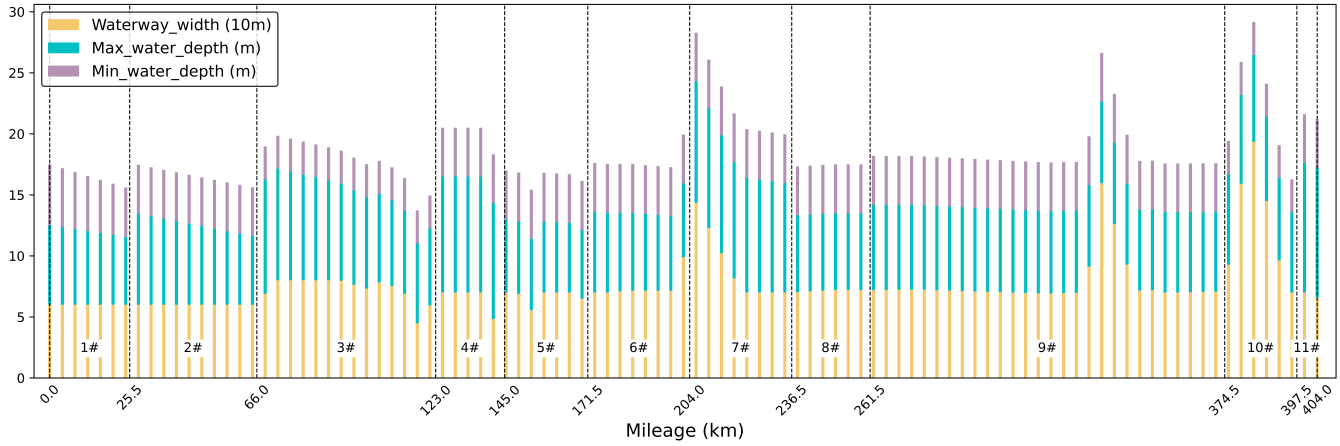

Figure 3. Water depth and waterway width of North Jiangsu Canal (data from the North Jiangsu Grand Canal Administration of Navigational Affairs). (The numbers ranging from 1# to 11# are the labels of segments).

Certain locks along the North Jiangsu Canal experience persistent congestion, with varying waiting and crossing policies for different vessel types. Cargo ships and containers constitute the primary vessel types navigating the canal. In a bid to bolster container traffic development, priority lock crossing privileges are afforded to containers in the North Jiangsu Canal. Figure 4 presents statistics pertaining to waiting times at locks along the canal for the year 2021. An analysis of Figure 4 indicates significant congestion occurring in select months at Shiqiao Lock, Shaobo Lock, and Huai'an Lock, while other locks experience infrequent congestion throughout the year.

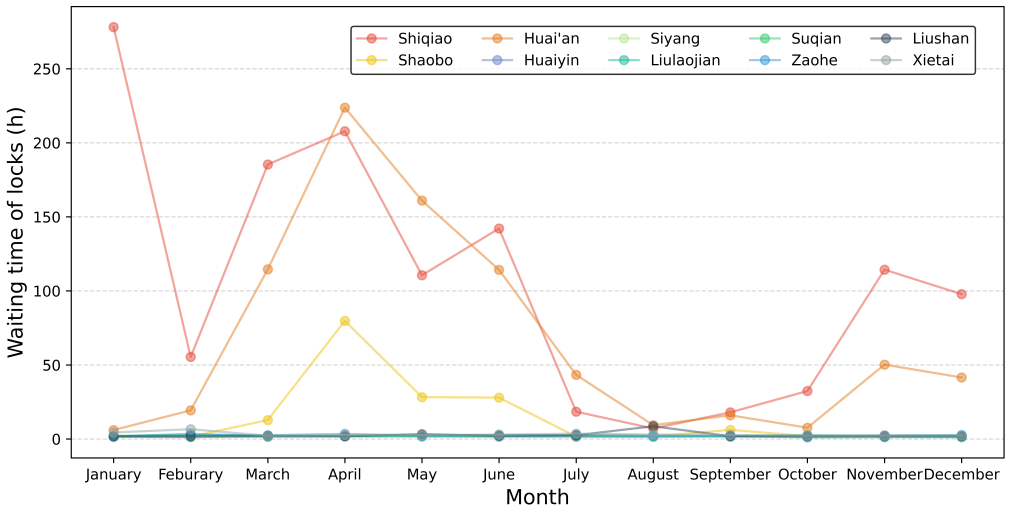

Figure 4. Statistics of the waiting time at locks on the North Jiangsu Grand Canal in 2021.

The North Jiangsu Canal predominantly accommodates small-tonnage and small-scale vessels, constituting the bulk of its maritime traffic. Utilizing statistical data spanning 350 days, from 1 January 2021 to 17 December 2021, a graphical representation (Figure 5) was generated to illustrate ship activities along the canal. Notably, Figure 5 highlights that the most prevalent category of ship length falls within the range of (40, 45], with a total of 7804 vessels, significantly surpassing other length categories. Furthermore, the overwhelming majority of ships exhibit a gross tonnage below 2000 tons.

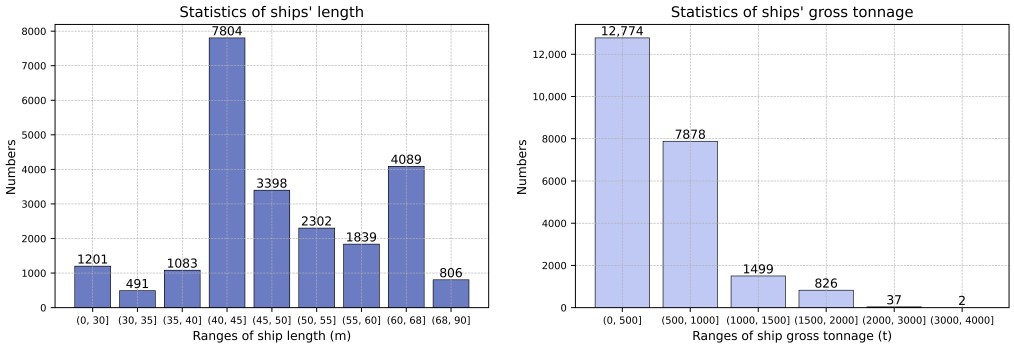

Figure 5. Statistics of ships sailing on the North Jiangsu Grand Canal in 2021.

4.2. Model Formulation

The selection of experimental ships adhered to the following three criteria, with their basic parameters outlined in Table 1:

- As depicted in Figure 5, the ship length categories (40, 45] and (60, 68] are both abundant and representative. Consequently, Ship 1 and Ship 3 were chosen for the experimental study.
- Given the emerging trend towards larger vessels, Ship 3 was selected to ensure the research remains forward-looking.
- Aligning with the green development trajectory of inland shipping, container ships hold significant importance and are granted priority lock crossing privileges. Hence, Ship 2 was chosen as a representative example of container ships.

As indicated in Table 1, the speed over ground and navigation mileage were acquired from the Automatic Identification System (AIS), while water depth and water flow velocity were obtained using a depth-sounder. Fuel consumption data were gathered using a fuel dipstick. The waiting time and waterway width were provided by the North Jiangsu Grand Canal Administration of Navigational Affairs. Notably, fuel consumption, water depth, and water flow velocity were recorded once per segment.

Table 1. Design parameters of the ship.

Parameters	Ship 1	Ship 2	Ship 3
Ship name	Haozhou 528	Runxingji 899	Jiangsu cargo 3001
Ship type	Bulk-cargo	Container	Bulk-cargo
Ship length (m)	42.8	62.0	75.1
Ship width (m)	8.0	13.0	14.8
Full load displacement (t)	637.6	2245.0	3041.5
Design draft (m)	2.96	3.45	3.60
Rated speed (r/min)	1500	1000	1200
Data capture	Automatic Identification System (AIS): speed over ground and navigation mileage. Depth-sounder: water depth, water flow velocity. Fuel dipstick: fuel consumption. Data from the North Jiangsu Grand Canal Administration of Navigational Affairs: waiting time and waterway width.		

The voyage data of the three experimental ships, which navigated the whole length of the North Jiangsu Canal, were recorded as three cases. Table 2 provides the relevant experimental data, including load, draft, sailing time, and start date during navigation. Due to the different start dates of the 3 cases, the water depth and water flow velocity of the same segment are different.

Table 3 presents the cases' data for the 11 segments, including mileage, waterway width, water flow velocity, water depth, and ship speed.

Table 2. Case settings of ship navigation experiments.

Case	Case Ship	Displacement (t)	Draft (m)	Sailing Time (h)	Start Date
Case 1	Ship 1	600	2.8	46.7	18 February 2022
Case 2	Ship 2	1050	2.1	43.2	20 January 2022
Case 3	Ship 3	2500	3.6	48.9	21 May 2021

Table 3. Data of 3 cases in 11 segments.

Segment		1#	2#	3#	4#	5#	6#	7#	8#	9#	10#	11#
Segment mileage (km)		25.5	40.5	57.0	22.0	26.5	32.5	32.5	25.0	113.0	23.0	6.5
Average waterway width (m)		60.0	60.0	74.8	67.9	68.1	78.8	70.0	72.0	73.3	114.7	68.7
Case 1	Water depth (m)	5.5	5.7	6.1	5.3	5.4	5.2	6.4	6.3	5.6	5.7	5.3
	water flow velocity (m/s)	0.4	0.2	0.0	0.4	0.5	0.7	0.1	0.0	0.3	0.4	0.4
	Ship speed (m/s)	1.97	2.06	2.65	2.03	2.03	2.35	2.13	2.19	1.93	2.11	2.48
Case 2	Water depth (m)	5.6	5.8	6.2	5.3	5.9	5.2	6.4	6.5	5.8	5.9	5.5
	water flow velocity (m/s)	0.2	0.1	0.0	0.3	0.2	0.4	0.0	0.0	0.3	0.1	0.2
	Ship speed (m/s)	2.70	2.67	2.45	2.48	2.44	2.75	2.93	3.11	2.00	2.29	2.28
Case 3	Water depth (m)	4.7	4.9	5.5	4.4	5.0	4.4	5.7	5.7	4.8	5.0	4.6
	water flow velocity (m/s)	1.8	1.8	1.2	2.0	1.5	1.9	0.9	1.0	1.9	1.3	1.7
	Ship speed (m/s)	2.16	2.09	2.21	2.06	2.12	2.24	2.33	2.23	1.89	1.86	1.82

In accordance with Equation (16), the engine speeds were computed as original data. Figure 6 depicts the relationship between engine speed and ship speed for segment 1# across the three cases, fitted using Equation (11) as a reference. The fitting coefficients for all segments are provided in Appendix A.

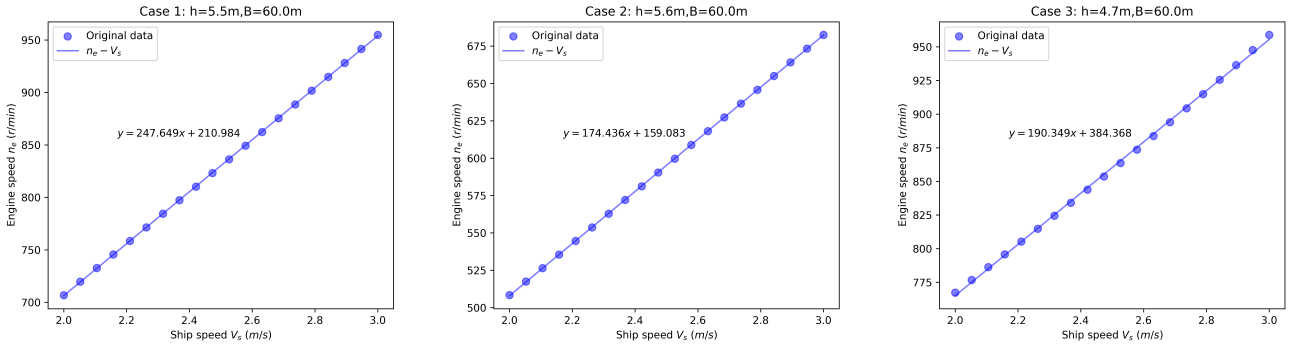

Figure 6. The relationship between engine speed and ship speed on segment 1# in the 3 cases.

The curves representing the main engine power and fuel consumption rate for the three ships were sourced from ship engine manuals. Employing Equations (17) and (18) for curve fitting, the fitting equations for $P_B - n_e$ and $g_e - n_e$ are depicted in Figure 7.

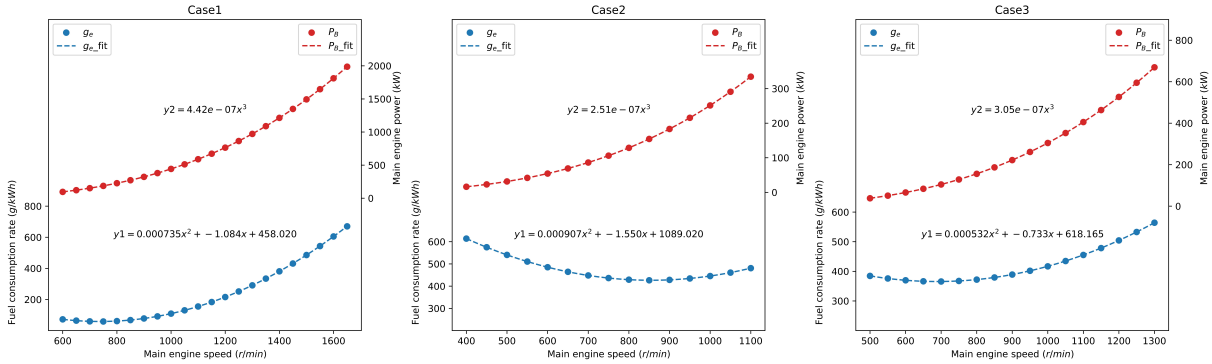

Figure 7. The fitting equations of main engine power and fuel consumption rate of the 3 ships.

Based on the ship crossing procedure in the North Jiangsu Canal, a total duration of 2.5 h was allocated from the ship's arrival at the lock to being notified to cross, including the time spent crossing the lock itself. Additionally, 0.5 h was designated for the ship to schedule its lock crossing appointment. Monthly average waiting times for crossing the 10 locks in the North Jiangsu Canal were obtained from the lock management office, with waiting times for ships in different segments adjusted according to the experimental voyage dates. The specified waiting times for each segment are detailed in Table 4. The total time indicated in Table 4 encompasses the duration from entering to exiting the North Jiangsu Canal. Notably, in Case 2, the experimental ship is a container vessel eligible for priority lock crossing at the North Jiangsu Canal, entailing a waiting time of zero.

Table 4. The setting of waiting time in each segment.

Segment	1#	2#	3#	4#	5#	6#	7#	8#	9#	10#	Total Time (h)
Case 1	2.22	1.85	2.19	2.57	1.07	1.89	1.47	7.60	1.94	35.38	110.6
Case 2	-	-	-	-	-	-	-	-	-	-	68.2
Case 3	2.67	1.84	3.40	1.95	1.76	1.90	1.81	226.56	69.77	217.81	589.6

Segment 11# has no waiting time as there are no locks at the end of the segment. "-" indicates no waiting time.

4.3. Results

The fuel consumption, as predicted by the ship fuel consumption model detailed in Section 3.2, was computed utilizing the experimental data from Tables 2 and 3. Figure 8 illustrates a comparison between the predicted and measured fuel consumption, while Table 5 presents evaluation metrics for the predictive performance across the three cases. Metrics such as MSE, RMSE, and MAE serve as indicators of model prediction accuracy. Table 5 indicates that Case 3 exhibits a higher error value compared to Case 1 and Case 2, attributed to Case 3's larger y-value. However, all three cases demonstrate R^2 values exceeding 0.97, and MAPE values below 10%. These findings suggest that the fuel consumption prediction model proposed in this study performs well overall.

Table 5. The evaluation indicators of the predicted effects in the 3 cases.

Case	MSE (kg)	RMSE (kg)	MAE	MAPE	R^2
Case 1	54.603	7.389	5.712	9.2%	0.977
Case 2	56.405	7.510	7.077	9.0%	0.984
Case 3	142.953	11.956	11.221	5.9%	0.994

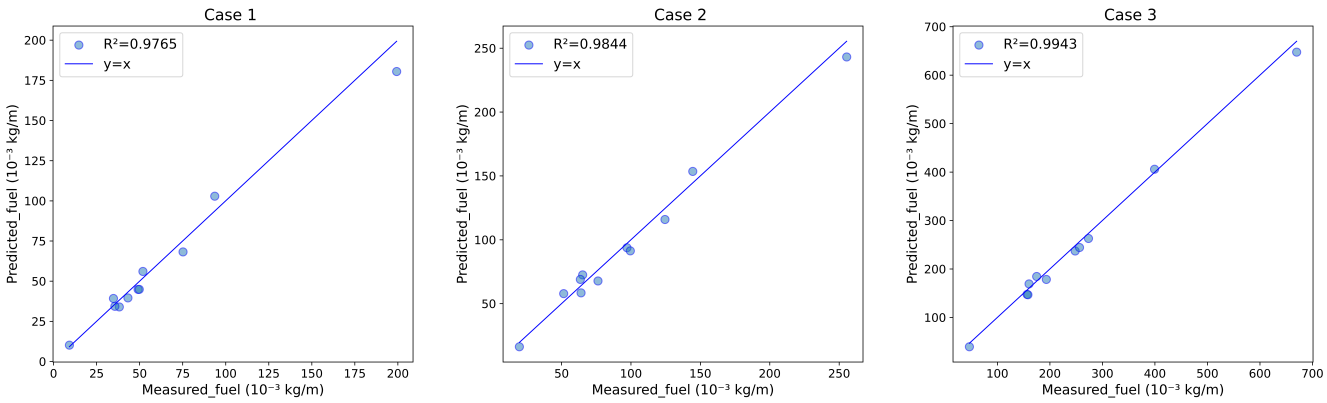

Figure 8. Comparison between predicted and measured fuel consumption in the 3 cases.

This paper employed two methods for speed optimization. The initial method computes the optimal speed for each segment, considering only the sailing time as a constraint. Conversely, the second method, introduced in this paper, incorporates waiting times into the calculation of optimal speed. Table 6 delineates the ship speeds in each segment before and after optimization, while Table 7 presents an analysis of the optimization effects for

the entire voyage. Additionally, Figure 9 provides a comparative visualization of fuel consumption before and after optimization across segments in the three cases.

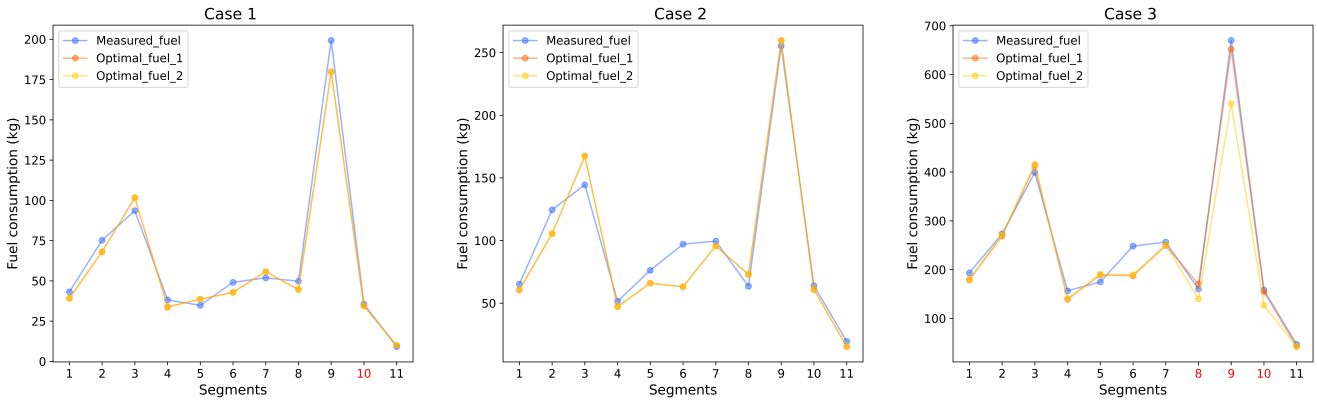

Figure 9. The ship fuel consumption before and after optimization for each segment of the 3 cases (the red x-axis scale indicates the segments where the waiting time exceeds the sailing time at the most fuel-efficient speed).

Table 6. The ship speeds before and after optimization (kn).

Segments	Case 1			Case 2			Case 3		
	Original	Optimal_1	Optimal_2	Original	Optimal_1	Optimal_2	Original	Optimal_1	Optimal_2
1#	3.84	3.05	3.05	5.25	4.23	4.23	4.19	4.21	4.26
2#	4.01	4.48	4.40	5.19	4.58	4.58	4.06	4.20	4.25
3#	5.16	4.79	4.73	4.77	5.69	5.69	4.30	4.42	4.47
4#	3.94	3.07	4.13	4.83	3.85	3.85	4.01	3.74	3.79
5#	3.95	3.07	3.07	4.74	4.56	4.56	4.12	4.27	4.32
6#	4.57	3.11	3.11	5.34	3.57	3.57	4.36	3.45	3.50
7#	4.14	4.68	4.62	5.70	6.31	6.31	4.52	4.67	4.72
8#	4.26	4.78	4.72	6.04	6.97	6.97	4.34	4.39	2.31
9#	3.75	4.48	4.39	3.89	4.26	4.26	3.67	3.71	1.92
10#	4.10	4.55	3.17	4.44	4.72	4.72	3.61	3.88	2.31
11#	4.82	3.07	3.07	4.43	4.14	4.14	3.55	3.88	3.93
Average speed	4.66	4.66	4.60	5.05	5.05	5.05	4.46	4.46	3.55

Table 7. Analysis of the optimization effects in the 3 cases.

Cause	Original	Optimal		Reduction		Reduced Rate	
		1	2	1	2	1	2
Case 1							
Fuel consumption (kg)	679.90	648.89	648.86	31.01	31.04	4.56%	4.78%
Carbon emissions (kg)	2179.76	2080.33	2080.25	99.43	99.51		
Case 2							
Fuel consumption (kg)	1061.00	1014.18	1014.18	46.82	46.82	4.41%	4.41%
Carbon emissions (kg)	3401.57	3251.45	3251.45	150.12	150.12		
Case 3							
Fuel consumption (kg)	2736.90	2645.33	2421.14	91.57	315.76	3.35%	11.54%
Carbon emissions (kg)	8774.50	8480.93	7762.17	293.57	1012.33		

4.4. Discussion

This paper conducts case studies involving three types of ships: a small-tonnage cargo ship (Ship 1), a container ship (Ship 2), and a large-tonnage cargo ship (Ship 3). The study applies two speed optimization methods to these cases and compares the optimization effects of a conventional approach with a method proposed in this paper. The calculation outcomes and their implications are discussed in the following parts.

Table 6 illustrates that longer waiting times lead to a decrease in the average ship speed. In Case 1, where the waiting time for segment 10# is 35.38 h, Ship 1 manages to sail at the

most fuel-efficient speed of 3.17 knots. However, this has a negligible impact on the overall average ship speed for the entire voyage. Conversely, Case 2, representing an experimental container ship with no waiting time, yields identical results for both optimization methods. While the average sailing time of Case 2 remains consistent with the original data, there are notable differences in the speed distribution across each segment. Notably, Case 3 encounters extended waiting times in segments 8#, 9#, and 10#, spanning durations of 226.56 h, 69.77 h, and 217.81 h, respectively. Ship 3 maintains the most fuel-efficient speeds on these segments, averaging 2.31, 1.92 and 2.31 knots, respectively. However, owing to the greater distance covered in segment 9#, Case 3 experiences a reduction in average speed of 0.91 knots.

Figure 9 highlights that the speed optimization method, which accounts for waiting time, leads to more substantial fuel savings in segments where the waiting time surpasses the sailing time at the most fuel-efficient speed. The comparative fuel consumption graphs for Case 1 and Case 2 depicted in Figure 9 demonstrate a similarity in the fuel consumption patterns after optimization using both methods. However, in Case 3, the second method exhibits superior optimization outcomes compared to the first method, particularly evident in segments 8#, 9#, and 10#. Conversely, in other segments, the fuel consumption curves for both methods largely overlap.

Table 7 illustrates that the speed optimization method, incorporating waiting time, can significantly enhance the overall fuel consumption optimization rate. In Case 1, utilizing the first and second methods of speed optimization reduces overall fuel consumption by 31.01 kg and 31.04 kg, respectively, corresponding to carbon emission reductions of 99.43 kg and 99.51 kg, resulting in optimization rates of 4.56% and 4.78%, respectively. For Case 2, the speed optimization method achieves 4.41% optimization, saving 46.82 kg of fuel and reducing carbon emissions by 150.12 kg. Similarly, in Case 3, the second method achieves 11.54% optimization, saving 315.76 kg of fuel and reducing carbon emissions by 1012.33 kg. This represents an 8.19% enhancement in the fuel consumption reduction rate, leading to 224.19 kg of fuel savings and a carbon emission reduction of 718.77 kg compared to the calculation using the first method.

Overall, these findings suggest that the speed optimization method proposed in this study effectively enhances optimization outcomes, yielding greater fuel consumption savings and emission reductions, particularly in segments where waiting time surpasses sailing time at the most fuel-efficient speed. However, when only one segment experiences such delays, the method's advantage over conventional approaches is less pronounced. It is therefore inferred that employing the speed optimization method considering waiting time can notably enhance optimization efficacy, particularly during peak periods of congestion at canal locks.

5. Conclusions

This paper investigates ship speed optimization within the context of canal navigation. A fuel consumption prediction model is developed to accommodate the narrow channels of the canal. Specifically, the study introduces a speed optimization model accounting for lock congestion that integrates waiting time for lock crossings. Three representative ships are examined through case studies. Our results indicate high predictive accuracy of the prediction model, with R^2 values exceeding 0.97 for all cases. The proposed speed optimization method enhances optimization rates by 8.19% to 11.54% in segments with prolonged waiting times. Furthermore, for single-segment scenarios, it achieves 4.78% optimization in fuel consumption and emissions, comparable to conventional methods. Overall, this study underscores the efficacy of incorporating waiting time considerations in speed optimization, particularly during peak lock congestion periods.

This research endeavors to elevate the energy efficiency and intelligence of ships navigating canals. However, it is crucial to underscore that additional validation of the model is imperative for practical deployment. Future investigations could broaden the scope of environmental factors considered in calculation methodologies to better reflect

real-world conditions. Moreover, incorporating ship navigation experiments across various months could provide deeper insights into the impact of waiting time on speed optimization efficacy. By embracing these avenues, future research can enhance the robustness and applicability of speed optimization models in canal shipping operations.

Author Contributions: Conceptualization, W.X., S.X. and N.Z.; data curation, W.X.; investigation, W.X., N.Z. and L.M.; methodology, W.X.; project administration, S.X. and J.L.; resources, J.L.; supervision, S.X. and J.L.; validation, W.X., N.Z. and L.M.; visualization, W.X.; writing—original draft, W.X.; writing—review & editing, W.X., S.X., N.Z. and K.Y. All authors have read and agreed to the published version of the manuscript.

Funding: This research was funded by the Postgraduate Research and Practice Innovation Program of Jiangsu Province (No. SJCX22_0059).

Institutional Review Board Statement: Not applicable.

Informed Consent Statement: Not applicable.

Data Availability Statement: Data are contained within the article.

Conflicts of Interest: The authors declare no conflicts of interest.

Abbreviations

The following abbreviations are used in this manuscript:

EU	European Union
IMO	International Maritime Organization
GHG	Greenhouse gas
VDR	Voyage Data Recorder
NSGA-II	Non-dominated Sorting Genetic Algorithm II
EEOI	Energy Efficiency Operational Indicator
PSO	Particle Swarm Optimization
GA	Genetic algorithm
MDO	Marine Diesel Oil
MSE	Mean square error
RMSE	Root mean square error
MAE	Mean absolute error
MAPE	Mean absolute percentage error
AIS	Automatic Identification System

Appendix A

The fitting coefficients of the relationship between engine speed and ship speed of all segments in the 3 cases are listed in Table A1.

Table A1. The fitting coefficients of $n_e - V_s$ of all segments in the 3 cases.

Segments	Case 1		Case 2		Case 3	
	b_1	b_2	b_1	b_2	b_1	b_2
1#	247.608	211.064	174.471	158.985	190.227	384.575
2#	247.207	209.982	167.682	172.248	183.249	397.313
3#	239.346	214.694	138.181	236.240	176.933	413.873
4#	244.398	214.243	183.678	143.654	213.730	344.415
5#	243.901	214.321	161.858	185.484	185.795	395.755
6#	238.806	218.378	188.873	136.442	227.896	323.462
7#	241.138	211.681	123.538	267.549	171.350	421.558
8#	240.401	212.798	110.602	296.381	172.194	420.817
9#	240.563	216.035	166.387	177.296	197.690	376.424
10#	230.460	224.151	162.645	183.210	200.860	377.209
11#	243.924	214.586	178.585	152.859	202.953	364.736

References

1. European Climate Law. Available online: https://climate.ec.europa.eu/eu-action/european-climate-law_en (accessed on 7 September 2023).
2. Kerry, J.; Mccarthy, G. *The Long-Term Strategy of the United States: Pathways to Net-Zero Greenhouse Gas Emissions by 2050*; The United States Department of State and the United States Executive Office of the President: Washington, DC, USA, 2021.
3. Zhang, Y.; Qiao, J. A ship performance and genetic algorithm-based decision support system for vessel speed optimisation of ocean route. *Int. J. Ship. Trans. Log.* **2023**, *17*, 107–145. [CrossRef]
4. Fan, A.; Xiong, Y.; Yang, L.; Zhang, H.; He, Y. Carbon footprint model and low-carbon pathway of inland shipping based on micro-macro analysis. *Energy* **2023**, *263*, 126150. [CrossRef]
5. Zhou, C.; Huang, H.; Liu, Z.; Ding, Y.; Xiao, J.; Shu, Y. Identification and analysis of ship carbon emission hotspots based on data field theory: A case study in Wuhan Port. *Ocean Coast. Manag.* **2023**, *235*, 106479. [CrossRef]
6. Yin, K.; Xu, S.; Zhao, Q.; Zhang, N.; Li, M. Effects of sea surface warming and sea-level rise on tropical cyclone and inundation modeling at Shanghai coast. *Nat. Hazards* **2021**, *109*, 755–784. [CrossRef]
7. Initial IMO GHG Strategy. Available online: https://www.imo.org/en/MediaCentre/HotTopics/pages/reducing-greenhouse-gas-emissions-from-ships.aspx (accessed on 14 May 2019).
8. Getting to Zero Coalition. Available online: https://www.globalmaritimeforum.org/getting-to-zero-coalition (accessed on 7 March 2020).
9. Jia, P.; Zhang, W.; Wenhao, E.; Sun, X. A refueling scheme optimization model for the voyage charter with fuel price fluctuation and ship deployment consideration. *J. Syst. Sci. Inf.* **2017**, *5*, 267–278. [CrossRef]
10. Zhao, W.; Wang, Y.; Zhang, Z.; Wang, H. Multicriteria Ship Route Planning Method Based on Improved Particle Swarm Optimization-Genetic Algorithm. *J. Mar. Sci. Eng.* **2021**, *9*, 357. [CrossRef]
11. Borén, C.; Castells-Sanabra, M.; Grifoll, M. Ship emissions reduction using weather ship routing optimisation. *Proc. Inst. Mech. Eng. Part M J. Eng. Marit. Environ.* **2022**, *236*, 856–867. [CrossRef]
12. Tanaka, M.; Kobayashi, K. A route generation algorithm for an optimal fuel routing problem between two single ports. *Int. Trans. Oper. Res.* **2022**, *26*, 529–550. [CrossRef]
13. Barreiro, J.; Zaragoza, S.; Diaz-Casas, V. Review of ship energy efficiency. *Ocean Eng.* **2022**, *257*, 111594. [CrossRef]
14. Ančić, I.; Vladimir, N.; Luttenberger, L.R. Energy efficiency of ro-ro passenger ships with integrated power systems. *Ocean Eng.* **2018**, *166*, 350–357. [CrossRef]
15. Fan, A.; Yang, J.; Yang, L.; Liu, W.; Vladimir, N. Joint optimisation for improving ship energy efficiency considering speed and trim control. *Transp. Res. D Transp. Environ.* **2022**, *113*, 103527. [CrossRef]
16. Nzualo, T.D.M.; de Oliveira, C.E.F.; Pérez, T.O.A.; González-Gorbeña, E.; Rosman, P.C.C.; Qassim, R.Y. Ship speed optimization in green approach to tidal ports. *Appl. Ocean Res.* **2021**, *115*, 102845. [CrossRef]
17. Wang, H.; Lang, X.; Mao, W.; Zhang, D.; Storhaug, G. Effectiveness of 2D optimization algorithms considering voluntary speed reduction under uncertain met ocean conditions. *Ocean Eng.* **2020**, *200*, 107063. [CrossRef]
18. Fan, A.; Wang, Z.; Sun, X.; Qu, X. Study of ship speed optimisation model and influencing factors based on different scenarios. *Shipbuild. China* **2021**, *62*, 162–171.
19. Yang, L.; Chen, G.; Zhao, J.; Rytter, N.G.M. Ship speed optimization considering ocean currents to enhance environmental sustainability in maritime shipping. *Sustainability* **2020**, *12*, 3649. [CrossRef]
20. Yan, X.; Wang, K.; Yuan, Y.; Jiang, X.; Negenborn, R.R. Energy-efficient shipping: An application of big data analysis for optimizing engine speed of inland ships considering multiple environmental factors. *Ocean Eng.* **2018**, *169*, 457–468. [CrossRef]
21. Fan, A.; Wang, Z.; Yang, L.; Wang, J.; Vladimir, N. Multi-stage decision-making method for ship speed optimisation considering inland navigational environment. *Proc. Inst. Mech. Eng. Part M J. Eng. Marit. Environ.* **2021**, *235*, 372–382. [CrossRef]
22. Tang, S.; Xu, S.; Gao, J.; Ma, M.; Liao, P. Effect of Service Priority on the Integrated Continuous Berth Allocation and Quay Crane Assignment Problem after Port Congestion. *J. Mar. Sci. Eng.* **2022**, *10*, 1259. [CrossRef]
23. Xia, F.; Chen, Y.; Wang, Z.; Mao, L. A method for determining the maintenance bottom width of restricted inland waterways coupled with multiple factors. *J. Water Resour. Water Trans. Eng.* **2018**, *235*, 48–54.
24. Elsherbiny, K.; Terziev, M.; Tezdogan, T.; Incecik, A.; Incecik, A. Numerical and experimental study on hydrodynamic performance of ships advancing through different canals. *Ocean Eng.* **2020**, *195*, 106696. [CrossRef]
25. Yu, Q.; Yuan, Z.; Zhou, C. Resistance performance of ships in grade III restricted channels. *J. Shanghai Inst. Ship. Sci.* **2014**, *37*, 23–27, 49.
26. Hu, Z.; Jing, Y.; Hu, Q.; Hu, Q.; Zhou, T.; Osman, M. Prediction of fuel consumption for enroute ship based on machine learning. *IEEE Access* **2019**, *7*, 119497–119505. [CrossRef]
27. Uyanık, T.; Karatuğ, C.; Arslanoğlu, Y. Machine learning approach to ship fuel consumption: A case of container vessel. *Transport. Res. D Trans. Environ.* **2020**, *84*, 102389. [CrossRef]
28. Li, X.; Sun, B.; Jin, J. Ding, J. Optimization of Container Ship Considering Route Segmentation and Weather Data Loading Turning Point-Time Segmentation Method. *J. Mar. Sci. Eng.* **2022**, *10*, 1835. [CrossRef]
29. Martić, I.; Degiuli, N.; Borčić, K.; Grlj, C.G. Numerical Assessment of the Resistance of a Solar Catamaran in Shallow Water. *J. Mar. Sci. Eng.* **2023**, *11*, 1706. [CrossRef]

30. Hadi, E.S.; Tuswan, T.; Azizah, G.; Ali, B.; Samuel, S.; Hakim, M. L.; Satrio, D. Influence of the canal width and depth on the resistance of 750 DWT Perintis ship using CFD simulation. *Brodogradnja* **2023**, *74*, 117–144. [CrossRef]
31. Fan, A.; Yang, J.; Yang, L.; Wu, D.; Vladimir, N. A review of ship fuel consumption models. *Ocean Eng.* **2022**, *264*, 112405. [CrossRef]
32. Yuan, Y.; Wang, K.; Yin, Q.; Yan, X. Review on ship speed optimization. *J. Traffic Trans. Eng.* **2020**, *20*, 18–34.
33. Orihara, H.; Tsujimoto, M. Performance prediction of full-scale ship and analysis by means of on-board monitoring. part 2: Validation of full-scale performance predictions in actual seas. *J. Mar. Sci. Technol.* **2018**, *23*, 782–801. [CrossRef]
34. Yan, R.; Wang, S.; Harilaos, P.H. Data analytics for fuel consumption management in maritime transportation: Status and perspectives. part 2: Validation of full-scale performance predictions in actual seas . *Transp. Res. Part E Log. Transp. Rev.* **2021**, *155*, 102489. [CrossRef]
35. Coraddu, A.; Oneto, L.; Baldi, F.; Anguita, D. Vessels fuel consumption forecast and trim optimisation: A data analytics perspective . *Ocean Eng.* **2017**, *130*, 351–370. [CrossRef]
36. Liu, B.; Gao, D.; Yang, P.; Hu, Y. An Energy Efficiency Optimization Strategy of Hybrid Electric Ship Based on Working Condition Prediction. *J. Mar. Sci. Eng.* **2022**, *10*, 1746. [CrossRef]
37. Lu, J.; Wu, X.; Wu, Y. The Construction and Application of Dual-Objective Optimal Speed Model of Liners in a Changing Climate: Taking Yang Ming Route as an Example. *J. Mar. Sci. Eng.* **2023**, *11*, 157. [CrossRef]
38. Psaraftis, H.N.; Kontovas, C.A. Ship speed optimization: Concepts, models and combined speed-routing scenarios. *Transport. Res. Part C Emerg. Technol.* **2022**, *14*, 52–69. [CrossRef]
39. Zhang, L.; Peng, X.; Liu, Z.; Wei, N.; Wang, F. An application of augmented Lagrangian differential evolution algorithm for optimizing the speed of inland ships sailing on the Yangtze River. *Int. J. Nav. Arch. Ocean Eng.* **2014**, *44*, 52–69. [CrossRef]
40. Spitzer, D. Resistance and economic speed of ships and tows in inland waterways. *J. Waterw. Port Coast. Ocean Eng.* **2021**, *147*, 04021033. [CrossRef]
41. Ma, Y.; Zhao, Y.; Yu, J.; Zhou, J.; Kuang, H. An interpretable gray box model for ship fuel consumption prediction based on the SHAP framework. *J. Mar. Sci. Eng.* **2023**, *11*, 1059. [CrossRef]
42. Fourth Greenhouse Gas Study. 2020. Available online: https://www.imo.org/en/OurWork/Environment/Pages/Fourth-IMO-Greenhouse-Gas-Study-2020.aspx (accessed on 26 March 2021).
43. Zhang, N.; Xu, S.; Mao, L.; Tang, S.; Yin, K. Fuzzy evaluation of inland ship lock service condition based on combination weighting and Matter-Element extension cloud model. *J. Mar. Sci. Eng.* **2023**, *11*, 757. [CrossRef]

Disclaimer/Publisher's Note: The statements, opinions and data contained in all publications are solely those of the individual author(s) and contributor(s) and not of MDPI and/or the editor(s). MDPI and/or the editor(s) disclaim responsibility for any injury to people or property resulting from any ideas, methods, instructions or products referred to in the content.